

Highly coherent light at 13 nm generated by use of quasi-phase-matched high-harmonic generation

X. Zhang, A. R. Libertun, A. Paul, E. Gagnon, S. Backus, I. P. Christov, M. M. Murnane, and H. C. Kapteyn

JILA, University of Colorado, Boulder, Colorado 80309-0440

R. A. Bartels

Department of Electrical and Computer Engineering, Colorado State University, Fort Collins, Colorado 80523-1373

Y. Liu and D. T. Attwood

Center for X-Ray Optics, Lawrence Berkeley National Laboratory, and Applied Science and Technology Graduate Group, University of California, Berkeley, Berkeley, California 94720

Received December 1, 2003

By measuring the fringe visibility in a Young's double pinhole experiment, we demonstrate that quasi-phase-matched high-harmonic generation produces beams with very high spatial coherence at wavelengths around 13 nm. To our knowledge these are the highest spatial coherence values ever measured at such short wavelengths from any source without spatial filtering. This results in a practical, small-scale, coherent, extreme-ultraviolet source that is useful for applications in metrology, imaging, and microscopy. © 2004 Optical Society of America

OCIS codes: 030.1640, 140.7090, 140.7240, 190.2620, 190.7110, 190.7220.

Highly coherent extreme-ultraviolet (EUV) sources are desirable for many applications in microscopies, metrology of optics for EUV lithography, EUV nonlinear optics, and in developing new types of nanoprobes. However, many EUV sources, such as synchrotrons and undulators¹ and high-harmonic generation (HHG) implemented using pulsed gas jets² generally produce partially coherent light that requires that one use spatial filtering to improve the coherence at the expense of photon flux. In recent work Bartels *et al.* demonstrated that EUV light produced by HHG in gas-filled hollow waveguides exhibits full spatial coherence at wavelengths around 30 nm.³ The extended propagation length in the hollow-waveguide geometry not only provides favorable phase-matching conditions to generate EUV light more efficiently but also improves the spatial coherence of the generated EUV beams. More recently, we demonstrated that, by periodically modulating the diameter of a hollow-core waveguide, quasi phase matching (QPM) of HHG can be implemented at wavelengths below 4 nm.^{4,5} The periodic modulations of the waveguide modulate the driving laser intensity in the waveguide, which in turn modulates the phase and amplitude of the EUV light, allowing QPM.

In this Letter we show that QPM HHG in modulated waveguides generates EUV beams with high spatial coherence at wavelengths around 13 nm. These measurements yield important information about nonlinear optics at short wavelengths. First, we measure what is to our knowledge the highest intrinsic spatial coherence of any EUV light source at such short wavelengths. Second, for applications of HHG that require very small (submicrometer) spot sizes, it will be significantly easier to use spatially coherent light at wavelengths shorter than 30 nm, because x-ray reflective optics, or x-ray diffractive optics, are much more efficient at 13 nm than at 30 nm.¹ Third, background gas absorption is significantly higher at

13 than at 30 nm. This might imply that the spatial coherence would be lower at 13 nm, because long interaction lengths are not possible. However, our measurements show a surprising need for interaction lengths >6 cm to obtain high spatial coherence, despite absorption lengths of 1–4 mm in Ne and He. Fourth, the shorter wavelength and lower flux at 13 nm compared with 30 nm, combined with the diverging wave front of the HHG light, makes the long-term EUV beam and phase stability much more critical at 13 nm than at 30 nm, as discussed in detail below. Fifth, we show that the use of modulated waveguides does not limit the EUV beam quality, despite the significant perturbation to the laser and EUV beams caused by the waveguide modulations and the refractive plasma. Finally, the development of coherent sources at 13 nm is important for next-generation EUV lithography.

In our experiments we focused sub-20-fs light pulses from a high-repetition-rate (2-kHz, ~1.5-mJ/pulse) Ti:sapphire laser system⁶ into a >6-cm-long modulated hollow-core waveguide filled with He (150-Torr) or Ne (70-Torr) gas. The peak intensity of the laser at the center of the beam was $\approx 5.2 \times 10^{14}$ W cm⁻². At these laser intensities Ne is approximately 2% ionized, whereas He is 0.2% ionized. The ~10% amplitude, 0.5-mm-period modulation of the 150- μ m inner-diameter hollow waveguide enhances phase-matched frequency conversion from the fundamental into high harmonics at higher photon energies than is possible using a simple, constant-diameter waveguide.

The pinhole pairs used for the coherence measurements were placed ~60 cm after the exit of the waveguide, where the EUV beam was ~1.5-mm diameter. This beam size is consistent with a small source diameter of 15–17 μ m and is also consistent with our theoretical estimation of a beam divergence of ~1.4 mrad. Given the known laser intensity within the waveguide, the waveguide transmission, and the cutoff rule for HHG,^{7,8} the laser intensity is below threshold for

generating harmonics at 13 nm for radii $>17\ \mu\text{m}$. The interference pattern was then recorded with an EUV CCD camera (Andor, Inc., $13.5\text{-}\mu\text{m}$ pixel size), placed $\sim 3\ \text{m}$ after the pinholes. At this distance the EUV beam diameter was $\sim 1\ \text{cm}$. Two $0.2\text{-}\mu\text{m}$ -thick zirconium filters in the beam path were used to eliminate the remaining 800-nm residual laser light.

To determine the spatial coherence of the EUV beams generated in the modulated hollow-core waveguide, we measure the visibility of the central fringes of the interference pattern.^{3,9} Because of the low divergence of the short-wavelength EUV beams from each pinhole, and the subsequent further separation of the Airy patterns as a result of the EUV beam wave-front tilt at the pinholes, even for very small ($<20\text{-}\mu\text{m}$) pinhole sizes the Airy patterns overlap in only a limited region to produce fringes. This, together with the relatively large bandwidth of the EUV beams, implies that only the intensity of the central fringes of the EUV interference pattern can be used to calculate the fringe visibility. The finite overlap region for fringe visibility measurements as a result of the diverging wave front of the EUV beam also limits the largest pinhole separation at which we can observe fringes to 60% of the beam diameter. Moreover, any EUV beam instability will phase and amplitude modulate the EUV light at the pinholes, reducing the fringe visibility measured in an integrated experiment. We note, however, that these are measurement limitations and should not prevent the use of this source for metrology and imaging.

Figure 1 shows typical images and intensity profile lineouts of interference patterns obtained for different pinhole sizes and separations, for an EUV beam generated by a 0.5-mm -period modulated waveguide filled with He at 110 Torr. Figures 1(a) and 1(b) correspond to fringe patterns obtained with $50\text{-}\mu\text{m}$ -diameter pinholes, placed 150 and $250\ \mu\text{m}$ apart, respectively, with acquisition times of 240 s (4.8×10^5 laser pulses). Figures 1(c) and 1(d) correspond to fringe patterns obtained with $20\text{-}\mu\text{m}$ -diameter pinholes, placed 300 and $450\ \mu\text{m}$ apart, respectively, with acquisition times of 1800 s (3.6×10^6 laser pulses). The excellent fringe contrast obtained even for the long-duration measurements shows that the spatial coherence of this EUV light source is highly stable over extended times. The long exposure times are required because of the high level of attenuation of the EUV beam by the pinholes, which transmit $<0.08\%$ of the EUV beam.

These symmetric pinhole measurements compare the spatial coherence of parts of the beam that are equidistant from the center. A question remains if there could exist random phase variations between portions of the beam at different annuli. However, this is highly unlikely for many reasons. First, modal averaging and guiding of the laser beam propagating in the fiber ensure good phase uniformity for both the laser and the EUV beams. Second, both far- and near-field EUV beam profiles exhibit Gaussian-like propagation, demonstrating that the EUV beam has a smooth and spherical wave front. Coupled with the pinhole measurements, these facts indicate good

spatial coherence over the entire EUV beam. Third, in previous measurements at 30 nm not only were pinhole measurements performed but also they demonstrated Gabor holography that would not be possible if the fiber introduced random phase variations in the EUV beam at different radii.³ Finally, waveform characterization techniques^{10,11} that are possible at longer wavelengths where the EUV flux is higher did not observe any random phase variations. However, flux limitations currently limit such techniques to the center 60% of the EUV beam even at these longer wavelengths.

Figure 2 shows the fringe visibility as a function of pinhole separation for EUV light generated with modulated waveguides filled with both He and Ne. Even for the most separated pinhole pairs, the fringe visibility is 0.9 or greater. Approximately 50% of the EUV beam energy is contained within the beam diameter represented by the largest separation. The slightly less than optimal fringe visibility obtained for the higher pinhole separation can be attributed to two main factors: first, the long integration time required to acquire the image because of the lower HHG flux at short wavelengths, and, second, the relatively low signal-to-noise ratio in the fringes as a result of the low overlap of the Airy disks (due to the diverging HHG wave front). The long integration times result in errors such as those introduced by any variation in the laser (and hence EUV) beam pointing. This will affect the relative intensity and the initial phase of the EUV light from each pinhole, reducing the fringe visibility for images with a long acquisition time.

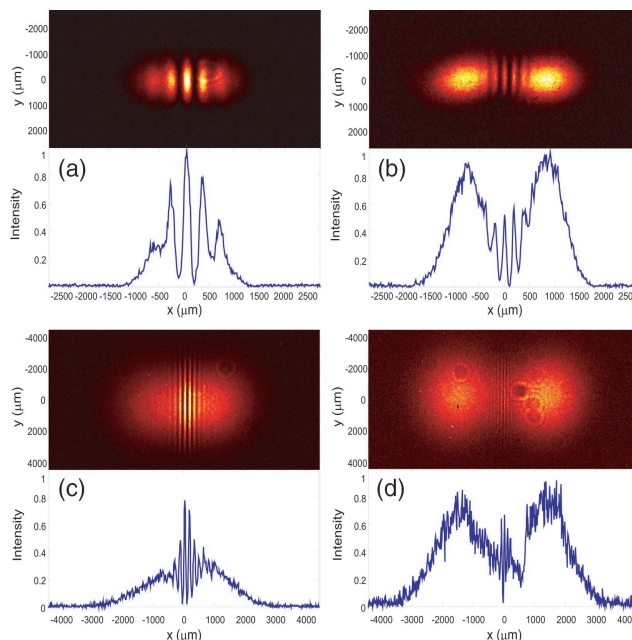


Fig. 1. Typical images (top) and intensity profiles (bottom) of the interference patterns from modulated waveguides filled with He at 150 Torr: (a), (b) $50\text{-}\mu\text{m}$ pinholes placed 150 and $250\ \mu\text{m}$ apart, with acquisition times of 240 s; (c), (d) $20\text{-}\mu\text{m}$ -diameter pinholes, placed 300 and $450\ \mu\text{m}$ apart, with acquisition times of 1800 s. The pinholes are centered on the EUV to ensure equal illumination.

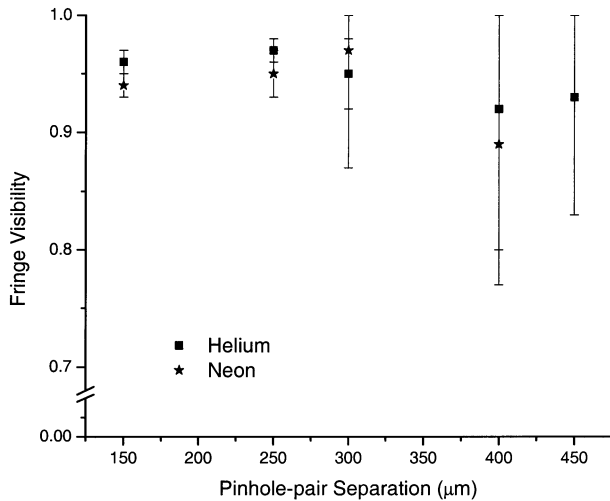


Fig. 2. Fringe visibility as a function of pinhole separation for EUV light generated with modulated waveguides filled with He and Ne.

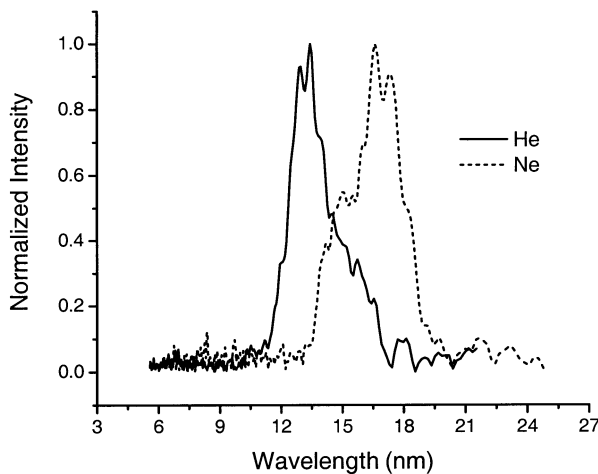


Fig. 3. Spectral envelopes of the EUV light obtained by the far-field interferogram Fourier-transform method for He- and Ne-filled waveguides. For He the spectrum spans harmonic orders 49–69, and for Ne the spectrum includes harmonic orders 41–59.

Figure 3 shows the result of applying the far-field interferogram Fourier-transform method¹² to the interferogram obtained with two 20- μm slits 400 μm apart. For this measurement slits were used instead of pinholes to increase the total transmitted light. For our conditions this method produces an approximate spectrum of the EUV light, because the diverging EUV beam introduces a wave-front tilt and also because the finite size of the slits limits the resolving power. Therefore, this approach gives an accurate central wavelength but overestimates the fractional bandwidth (for slits of width d and separation s , the resolving power is given by $0.8 d/s$). From these data the spectrum of the light generated in He is centered at 13 nm and has a fractional bandwidth of ~ 0.15 . By use of Ne, the EUV light is centered at 17 nm, with a fractional bandwidth of ~ 0.3 . Both spectra contain approximately ten harmonic orders.

We note that the relatively large bandwidth of the radiation, together with the long acquisition times, makes measurement of 100% fringe contrast difficult even for the case of the smallest pinhole-separation interference pattern. Each image shown in Fig. 1 is a superposition of the interference patterns of all ten harmonic orders generated in the waveguide, so only the central fringe of each of the ten interference patterns will be perfectly superimposed.

In summary, we have measured very high spatial coherence of EUV radiation in the wavelength range 11–19 nm generated in modulated hollow waveguides. We have experimentally demonstrated that the EUV light generated with this waveguide geometry is coherent across most of the EUV beam for long ($>6\text{-cm}$) interaction lengths. To our knowledge, this is the highest spatial coherence ever obtained directly from a light source without spatial filtering at such short wavelengths. Furthermore, the high fringe visibility observed even for images with long acquisition time demonstrates the intrinsic stability and usefulness of the QPM HHG source.

The authors gratefully acknowledge support for this work from U.S. Department of Energy NNSA grant DE-FG03-02NA00063 and by the Engineering Research Centers Program of the National Science Foundation under NSF Award Number EEC-0310717. A. R. Libertun's e-mail address is arl@colorado.edu.

References

1. D. T. Attwood, *Soft X-Rays and Extreme Ultraviolet Radiation: Principles and Applications* (Cambridge U. Press, Cambridge, England, 1999).
2. T. Ditmire, E. T. Gumbrell, R. A. Smith, J. W. G. Tisch, D. D. Meyerhofer, and M. H. R. Hutchinson, *Phys. Rev. Lett.* **77**, 4756 (1996).
3. R. A. Bartels, A. Paul, H. Green, H. C. Kapteyn, M. M. Murnane, S. Backus, I. P. Christov, Y. Liu, D. T. Attwood, and C. Jacobsen, *Science* **297**, 376 (2002).
4. A. Paul, R. A. Bartels, R. Tobey, H. Green, S. Weiman, I. P. Christov, H. C. Kapteyn, M. M. Murnane, and S. Backus, *Nature* **421**, 51 (2003).
5. E. A. Gibson, A. Paul, N. Wagner, R. Tobey, D. Gaudiosi, S. Backus, I. P. Christov, A. Aquila, E. M. Gullikson, D. T. Attwood, M. M. Murnane, and H. C. Kapteyn, *Science* **302**, 95 (2003).
6. S. Backus, R. Bartels, S. Thompson, R. Dollinger, H. C. Kapteyn, and M. M. Murnane, *Opt. Lett.* **26**, 465 (2001).
7. K. C. Kulander, K. J. Schafer, and J. L. Krause, in *Super-Intense Laser-Atom Physics*, B. Piraux, A. L'Huillier, and K. Rzazewski, eds., Vol. 316 of NATO Advanced Science Institutes Series (Plenum, New York, 1993), pp. 95–110.
8. M. Lewenstein, Ph. Balcou, M. Y. Ivanov, A. L'Huillier, and P. B. Corkum, *Phys. Rev. A* **49**, 2117 (1994).
9. B. J. Thompson and E. Wolf, *J. Opt. Soc. Am.* **47**, 895 (1957).
10. D. G. Lee, J. J. Park, J. H. Sung, and C. H. Nam, *Opt. Lett.* **28**, 480 (2003).
11. L. LeDéroff, P. Salières, B. Carré, D. Joyeux, and D. Phalippou, *Phys. Rev. A* **61**, 43802 (2000).
12. R. A. Bartels, A. Paul, M. Murnane, H. C. Kapteyn, and S. Backus, *Opt. Lett.* **27**, 707 (2002).